

Saccharomyces cerevisiae as a Host for Chondroitin Production

Márcia R. Couto ¹, Joana L. Rodrigues ^{1,2,*}, Oscar Dias ^{1,2} and Lígia R. Rodrigues ^{1,2}

¹ CEB—Centre of Biological Engineering, University of Minho, 4710-057 Braga, Portugal; marciacouto93@gmail.com (M.R.C.); odias@ceb.uminho.pt (O.D.); lrnr@deb.uminho.pt (L.R.R.)

² LABBELS—Associate Laboratory, 4710-057 Braga, Portugal

* Correspondence: joanarodrigues@deb.uminho.pt; Tel.: +351-253604402

Abstract: Chondroitin is a glycosaminoglycan that has gained widespread use in nutraceuticals and pharmaceuticals, mainly for treating osteoarthritis. Traditionally, it has been extracted from animal cartilage but recently, biotechnological processes have emerged as a commercial alternative to avoid the risk of viral or prion contamination and offer a vegan-friendly source. Typically, these methods involve producing the chondroitin backbone using pathogenic bacteria and then modifying it enzymatically through the action of sulfotransferases. Despite the challenges of expressing active sulfotransferases in bacteria, the use of eukaryotic microorganisms is still limited to a few works using *Pichia pastoris*. To create a safer and efficient biotechnological platform, we constructed a biosynthetic pathway for chondroitin production in *S. cerevisiae* as a proof-of-concept. Up to 125 mg/L and 200 mg/L of intracellular and extracellular chondroitin were produced, respectively. Furthermore, as genome-scale models are valuable tools for identifying novel targets for metabolic engineering, a stoichiometric model of chondroitin-producing *S. cerevisiae* was developed and used in optimization algorithms. Our research yielded several novel targets, such as uridine diphosphate (UDP)-*N*-acetylglucosamine pyrophosphorylase (*QR11*), glucosamine-6-phosphate acetyltransferase (*GNA1*), or *N*-acetylglucosamine-phosphate mutase (*PCMI*) overexpression, that might enhance chondroitin production and guide future experimental research to develop more efficient host organisms for the biotechnological production process.

Keywords: chondroitin; *Saccharomyces cerevisiae*; metabolic models; metabolic engineering



Citation: Couto, M.R.; Rodrigues, J.L.; Dias, O.; Rodrigues, L.R.

Saccharomyces cerevisiae as a Host for Chondroitin Production. *SynBio* **2024**, *2*, 125–141. <https://doi.org/10.3390/synbio2020008>

Academic Editor: Yasuo Yoshikuni

Received: 15 January 2024

Revised: 25 February 2024

Accepted: 22 March 2024

Published: 3 April 2024



Copyright: © 2024 by the authors. Licensee MDPI, Basel, Switzerland. This article is an open access article distributed under the terms and conditions of the Creative Commons Attribution (CC BY) license (<https://creativecommons.org/licenses/by/4.0/>).

1. Introduction

Chondroitin is a glycosaminoglycan that naturally occurs in animals, in different concentrations, and in different sulfation patterns, percentages, and structure ratios, according to the tissue where it is present [1]. Unsulfated or fructosylated forms of this compound also exist in some pathogenic bacteria as a capsular constituent [2]. Chondroitin has been mainly used in nutraceuticals, pharmaceuticals, and veterinary supplements for osteoarthritis treatment and joint protection, but also in ophthalmological solutions and devices. Its biological activity varies according to its sulfonation pattern, therefore making it versatile and useful in a wide range of other potential applications [1]. The biotechnological production of chondroitin is generally based on cultivating the pathogenic bacteria *Escherichia coli* O5:K4:H4, which naturally produces a fructosylated form of chondroitin [3]. Many efforts have been made to engineer chondroitin production using safer microorganisms [4–7]; however, the yield did not meet the growing demand. Furthermore, eukaryotic microorganisms remain relatively unexplored, with a single work using *Pichia pastoris* for chondroitin production [8]. Nevertheless, eukaryotic microorganisms are particularly interesting for chondroitin production because of their ability to perform post-translational modifications, unlike prokaryotic organisms such as *E. coli*. In fact, glycosylation and correct folding are required for animal sulfotransferases to become active and perform the sulfonation of the chondroitin backbone [9], which makes the correct expression of these proteins challenging, especially in prokaryotic hosts [10]. *S. cerevisiae* has been one of the

most widely used microorganisms for industrial biotechnological production of several compounds. Its broad use as a host in metabolic engineering is related to several key factors. These include its rapid and robust growth, its ease of genetic manipulation for recombinant protein expression, and its ability to perform post-translational modifications, including glycosylation, as well as its proficiency in properly folding recombinant proteins [11–13]. Therefore, it can be an interesting host for the production of chondroitin.

Genome-scale metabolic models (GEMs) are powerful resources that consist in the representation of the entire metabolic network of a biological system, including enzymes, metabolites, reactions, genes, and their associations, containing information on stoichiometry, compartmentalization, and biomass composition [14]. The use of these models to evaluate the organism biological capabilities requires the representation of the biochemical conversions following a stoichiometric matrix representation containing the stoichiometric coefficients for each metabolite in each reaction, where reactions are the columns and the metabolites the rows [14,15]. Constraint-based modelling assumes that cells operate in a steady-state, meaning that the metabolites may not be accumulated, and by applying flux constraints through upper and lower bounds, this matrix is transformed into a system of linear equations which can be used to calculate the flux of each reaction [14,15]. As this represents an undetermined system, a biological relevant reaction, usually biomass production, is used as the objective function to formulate a linear problem that can be solved using mathematical programming [14]. Manipulating the reaction bounds allows the simulation of environmental conditions or genetic modifications such as knockouts [16]. Applying evolutionary algorithms is a common strategy in strain design for identifying targets for metabolic engineering. Additionally, other information can be integrated with GEMs such as regulatory, kinetics, and omics data to improve the predictive power of these models in specific conditions [17].

As GEMs provide a systems biology framework for phenotype simulation, they have wide applications in metabolism studying, identification of novel targets for metabolic engineering, disease understanding, and drug target identification [14,18–22]. In particular, the industrial applications of GEMs are the most reported as they have been used for enhancing the biotechnological production of several compounds, either endogenous or heterologous, such as dicarboxylic acids [23–29], alcohols [30–32], amino acids [33–35], polymers [36–39], antibiotics [40,41], and polyphenols [42–44].

This study explores the potential of chondroitin production in *S. cerevisiae* using synthetic biology and metabolic engineering strategies. Furthermore, using a budding yeast GEM, in silico flux analysis was employed, as well as evolutionary algorithms, to identify novel targets for improving chondroitin titers in the future.

2. Results

2.1. Heterologous Production of Chondroitin in *S. cerevisiae*

The reports on the use of eukaryotic microorganisms for chondroitin or chondroitin sulfate production are still very limited. The first study in this area used *P. pastoris* to express the sulfotransferases, which were then used to sulfate a chondroitin backbone produced by an engineered *Bacillus subtilis* strain [7]. Subsequently, the same group engineered a *P. pastoris* strain that was able to produce 190 mg/L of chondroitin, and upon addition of the sulfonation module, 182 mg/L of chondroitin sulfate [8]. This work is the only one to have used a eukaryotic microorganism for chondroitin production. More recently, the same group also engineered a *P. pastoris* strain to produce another complex glycosaminoglycan, namely heparin [45].

We aimed to assess the potential of the widely used eukaryotic microorganism, *S. cerevisiae*, as a host for biotechnological production of chondroitin. For the first step of the pathway, uridine diphosphate (UDP)-glucose 6-dehydrogenase (UGD) from *Zymomonas mobilis* (Zmugd) was selected. Previously, we tested this enzyme and concluded it was the best option, as it presented higher enzymatic activity in in vivo experiments among a number of enzymes [46]. For the other steps catalyzed by UDP-N-acetylglucosamine

4-epimerase, UAE and chondroitin synthase/polymerase, CHSY, two set of genes were tested. In one case, *kfoA* and *kfoC* from pathogenic *E. coli* O5:K4:H4, encoding UAE and CHSY, respectively, were tested. These genes were previously used to efficiently construct the pathway in non-pathogenic *E. coli* and other hosts, making them a safer choice for obtaining positive results. In the other case, UAE from *Giardia intestinalis* (*Giuae*) and CHSY from *Bos taurus* (*Btchsy*) were tested. These two genes were never used for biotechnological production of chondroitin but presented promising activity results in characterization tests [47–50]. The three genes necessary to produce chondroitin in *S. cerevisiae* (*UGD*, *UAE*, and *CHSY* genes) were cloned in pSP-GM1 and pBEVY. However, after transforming the constructed plasmids carrying the designed pathways for chondroitin production, the transformants were rare, and after picking colonies from agar plates, some colonies were not able to grow on pre-inoculum liquid medium. Figure 1 shows the performance on chondroitin production by the tested transformants.

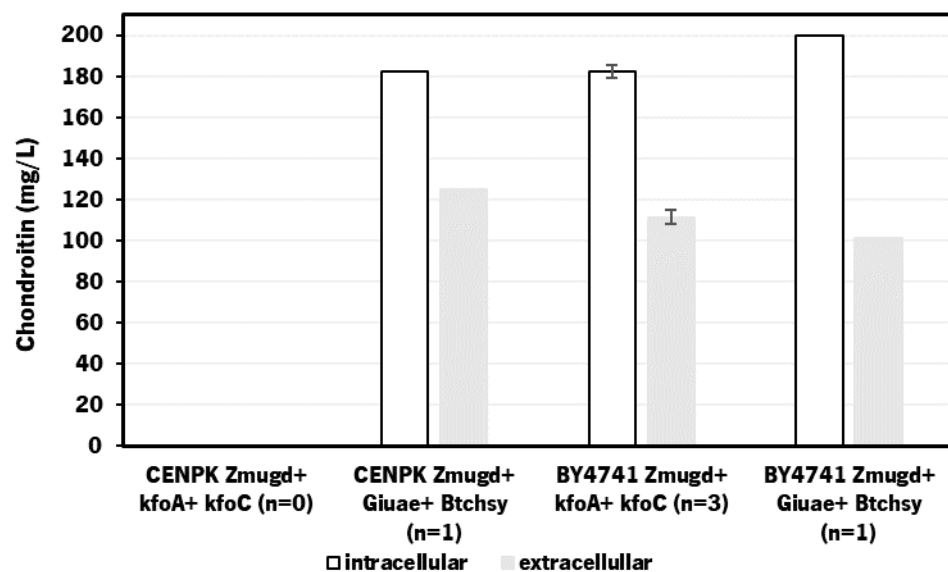


Figure 1. Chondroitin production in engineered *Saccharomyces cerevisiae* CEN.PK2-1C (CENPK) and BY4741 strains. *Btchsy*: chondroitin synthase/polymerase (CHSY) from *Bos taurus*; *Giuae*: UDP-*N*-acetylglucosamine 4-epimerase (UAE) from *Giardia intestinalis*; *kfoA* and *kfoC*: UAE and CHSY, respectively, from *Escherichia coli* K4 (serotype O5:K4(L):H4); *Zmugd*: uridine diphosphate (UDP)-glucose 6-dehydrogenase (UGD) from *Zymomonas mobilis*.

S. cerevisiae is often used as a host organism for the expression of heterologous genes and can carry multiple plasmids simultaneously. However, introducing multiple plasmids into a yeast cell can have various effects on cell growth and physiology. Some potential problems that may arise include the following: (a) metabolic burden—the presence of multiple plasmids and the expression of heterologous genes can impose an additional metabolic burden on the host yeast cell, resulting in reduced growth rates and compromised cell viability; (b) competitive replication—plasmids often compete for limited cellular resources during replication, leading to instability and loss of one or both plasmids over time, leading to a heterogeneous population of cells with varying plasmid content; (c) induced stress responses—the expression of foreign genes may induce stress responses in the host cell, triggering various regulatory mechanisms that can affect cellular homeostasis and growth.

To overcome these potential issues, several strategies can be employed, including the following: (a) balanced expression of genes—fine-tuning the expression levels of multiple genes can help alleviate the metabolic burden and minimize adverse effects on cell growth and physiology; (b) strain engineering—using engineered yeast strains with improved capabilities for handling metabolic stress or expressing foreign genes can help mitigate the negative impacts on cell growth; (c) adaptative laboratory evolution—improving the performance of microbial strains under specific conditions by subjecting a population of microorganisms to prolonged periods of growth under controlled selective pressure, allows the natural selection of beneficial mutations that may result in yeast strains adapted to efficiently manage the additional genetic load. The combination of these strategies might result in robust yeast strains capable of efficiently carrying multiple plasmids and expressing heterologous genes without compromising growth or productivity. Additionally, the heterologous genes can be integrated into the yeast genome, which can improve the stability of expression and reduce heterogeneity [51]. This is often seen as the next step after testing gene expression in plasmids, which provide higher copy numbers for validation of the expression.

Despite obtaining few viable colonies in transformations, the strains, herein constructed, were able to produce intracellular chondroitin between 182 and 200 mg/L, and extracellular chondroitin between 101 and 125 mg/L, with no significant differences observed between the various constructs and strains.

Comparing to the other work describing chondroitin production using *P. pastoris* [8], the genes used for the chondroitin production module were *kfoC*, *kfoA* (from *E. coli* K4), and *tuaD* (UDP-glucose dehydrogenase from *B. subtilis*) and, in a first attempt, only 5.5 mg/L chondroitin was obtained. After further codon-optimization of the genes, the chondroitin production increased to 189.8 mg/L, being in the same range of the chondroitin production achieved in this study. Therefore, our proof-of-concept study demonstrates that *S. cerevisiae* can be a suitable host to produce chondroitin. In the future, the integration of the three genes of the heterologous pathway should be considered to improve the stability and decrease the heterogeneity, as previously mentioned.

2.2. Bioinformatics Tool for Identification of Gene Targets

A model of *S. cerevisiae* metabolism was modified to include the heterologous reactions, intermediates, and genes required for chondroitin production. At that stage, optimizations for improving chondroitin production could not find any solution, either searching for knockout or under- and overexpression targets. One possible hypothesis for this was that biomass growth was not being properly coupled with product formation. We then realized that the original biomass equation did not predict the inclusion of chitin. Even though *S. cerevisiae* is reported to have a minimal amount of chitin, its presence might still be necessary for essential functions related to cell wall integrity and other processes, as suggested by the finding that simultaneous knockout of all three chitin synthase genes is lethal in yeast [52]. Therefore, based on the literature [53–55], the biomass equation was corrected to include 1% chitin. This was achieved by adjusting the reaction stoichiometry in the model to maintain the stoichiometric coefficients of other compounds, while including the necessary stoichiometric coefficient to achieve the desired percentage of chitin (Table 1). As chitin is an important intervenient in pathways related with chondroitin precursors, this adjustment could result in optimization results.

Table 1. Intermediates and their stoichiometric values in growth equation in the model yeast-GEM 8.4.2 before and after including 1% of chitin.

| Compound ID Code | Compound Name | Template Model | | Corrected Model 1% Chitin | |
|------------------|----------------------------------|----------------|----------------|---------------------------|----------------|
| | | Stoichiometry | Percentage (%) | Stoichiometry | Percentage (%) |
| s_0001_ce | (1→3)-β-D-glucan [cell envelope] | 0.748514964 | 33.88 | 0.748514964 | 33.54 |
| s_0004_ce | (1→6)-β-D-glucan [cell envelope] | 0.250091654 | 11.32 | 0.250091654 | 11.21 |
| s_0773_c | glycogen [cytoplasm] | 0.361414528 | 16.36 | 0.361414528 | 16.20 |
| s_1107_c | mannan [cytoplasm] | 0.710939625 | 32.18 | 0.710939625 | 31.86 |
| s_1520_c | trehalose [cytoplasm] | 0.138275712 | 6.26 | 0.138275712 | 6.20 |
| s_0509_c | chitin [cytoplasm] | 0 | 0.00 | 0.022313288 | 1.00 |

In fact, after performing these modifications, the optimization using evolutionary algorithms in OptFlux was able to find multiple solutions. The solutions with the best biomass-product coupled yield (BPCY) are shown in Table 2.

Table 2. Optimization of chondroitin production in yeast-GEM_c model using OptFlux. The optimization algorithm for under and overexpression identification was run three times. The predicted phenotype for the unmodified and modified strains (from the resulting solutions with highest biomass-product coupled yield, BPCY) are shown. The growth rate and chondroitin production rate are presented in units of h^{-1} and $\text{mmol/g}_{\text{DW}}/\text{h}$, respectively. BPCY is calculated by OptFlux by multiplying biomass by product and then dividing by substrate consumed (in all cases being $10 \text{ mmol/g}_{\text{DW}}/\text{h}$), as predicted by pFBA simulation. Flux variability analysis (FVA) results are shown as minimum and maximum chondroitin obtained through pFBA for fixed biomass.

| Solution | BPCY | Genes Modified | | Predicted Phenotype (pFBA) | | FVA | |
|----------|---------|------------------|-----------------|-----------------------------|---|---|---|
| | | Under Expression | Over Expression | Biomass (h^{-1}) | Chondroitin Flux ($\text{mmol/g}_{\text{DW}}/\text{h}$) | Minimum Chondroitin Flux ($\text{mmol/g}_{\text{DW}}/\text{h}$) | Maximum Chondroitin Flux ($\text{mmol/g}_{\text{DW}}/\text{h}$) |
| - | - | - | - | 0.8612 | 0.0000 | - | - |
| 1 | 0.04375 | - | <i>QR11</i> | 0.7317 | 0.5980 | 0.5980 | 0.9358 |
| 2 | 0.04375 | - | <i>GNA1</i> | 0.7317 | 0.5980 | 0.5980 | 0.9358 |
| 3 | 0.04375 | - | <i>PCM1</i> | 0.7317 | 0.5980 | 0.5980 | 0.9358 |

Gene descriptions: *GNA1*—glucosamine-6-phosphate acetyltransferase; *PCM1*—*N*-acetylglucosamine-phosphate mutase; *QR11*—uridine diphosphate-*N*-acetylglucosamine pyrophosphorylase.

Despite allowing for ten modifications, the solutions pointed to single modifications, namely the overexpression of one of the genes involved in the production of chondroitin precursors, *QR11*, *GNA1*, or *PCM1* (expression values of 32). *GNA1* encodes glucosamine-6-phosphate acetyltransferase, which catalyzes *N*-acetylglucosamine 6-phosphate synthesis, from glucosamine 6-phosphate and acetyl-coenzyme A (acetyl-CoA). *PCM1*, encoding *N*-acetylglucosamine-phosphate mutase, is responsible for converting *N*-acetylglucosamine 6-phosphate to *N*-acetylglucosamine 1-phosphate. *QR11*, encoding UDP-*N*-acetylglucosamine pyrophosphorylase, is responsible for the formation of UDP-*N*-acetylglucosamine. Figure 2 shows a schematic representation of the metabolism of *S. cerevisiae* that is involved in the biosynthetic production of chondroitin and the possible competing pathways.

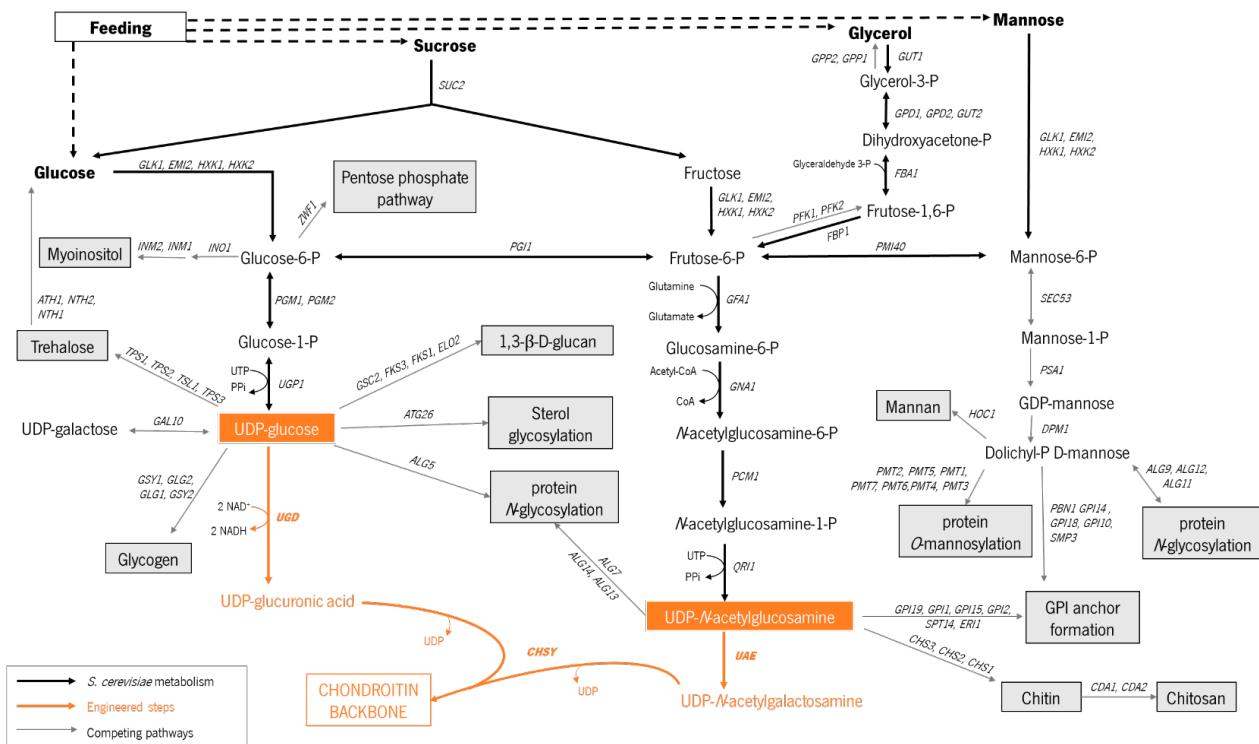


Figure 2. Pathways involved in chondroitin production in engineered *Saccharomyces cerevisiae*, and competing pathways that redirect the metabolic flux from chondroitin precursors. Compound abbreviations: CoA—coenzyme A; NAD⁺—nicotinamide adenine dinucleotide, oxidized form; NADH—nicotinamide adenine dinucleotide, reduced form; PPi—diphosphate; GPI—glycosylphosphatidylinositol; UDP—uridine diphosphate; UTP—uridine triphosphate; Gene descriptions: *ALG11*—Alpha-1,2-mannosyltransferase; *ALG12*—Alpha-1,6-mannosyltransferase; *ALG9*—mannosyltransferase; *ALG5*—UDP-glucose:dolichyl-phosphate glucosyltransferase; *ATH1*—acid trehalase; *ATG26*—UDP-glucose:sterol glucosyltransferase; *CDA1*, *CDA2*—chitin deacetylase; *CHS1*, *CHS2*, *CHS3*—chitin synthases; *CHSY*—chondroitin synthase; *DPM1*—dolichol phosphate mannosyltransferase; *EMI2*—hexokinase; *ERI1*—endoplasmic reticulum-associated Ras Inhibitor; *FBA1*—fructose 1,6-bisphosphate aldolase; *FBP1*—fructose-1,6-bisphosphatase; *FKS1*, *FKS3*—1,3-β-D-glucan synthase; *GAL10*—UDP-glucose-4-epimerase; *GLG1*, *GLG2*—glycogenin glucosyltransferase; *GLK1*—glucokinase; *GNA1*—glucosamine-6-phosphate *N*-acetyltransferase; *GPD1*, *GPD2*—glycerol-3-phosphate dehydrogenases; *GPI1*, *GPI10*, *GPI14*, *GPI15*, *GPI18*, *GPI19*—GPI anchor proteins; *GPP1*, *GPP2*—glycerol-3-phosphate phosphatases; *GSC2*—1,3-β-glucan synthase; *GSY1*, *GSY2*—glycogen synthases; *GUT1*—glycerol kinase; *GUT2*—glycerol-3-phosphate dehydrogenase; *HXX1*, *HXX2*—hexokinases; *INO1*—inositol-3-phosphate synthase; *INM1*, *INM2*—inositol monophosphatases; *NTH1*, *NTH2*—neutral trehalases; *PBN1*—glycosylphosphatidylinositol-mannosyltransferase I; *PCM1*—*N*-acetylglucosamine-6-phosphate mutase; *PFK1*, *PFK2*—phosphofructokinase; *PGI1*—phosphoglucose isomerase; *PMT1*, *PMT2*, *PMT3*, *PMT4*, *PMT5*, *PMT6*, *PMT7*—protein *O*-mannosyltransferases; *PSA1*—guanosine diphosphate(GDP)-mannose pyrophosphorylase; *QRI1*—UDP-*N*-acetylglucosamine pyrophosphorylase; *SEC53*—phosphomannomutase; *SMP3*—alpha 1,2-mannosyltransferase; *SPT14*—UDP-glycosyltransferase; *SUC2*—invertase; *TPS1*—trehalose-6-phosphate synthase; *TPS2*—trehalose-phosphatase; *TPS3*—trehalose-6-phosphatase; *UAE*—UDP-*N*-acetylglucosamine 4′-epimerase; *UGD*—UDP-glucose 6-dehydrogenase; *ZWF1*—glucose-6-phosphate dehydrogenase.

The overexpression of genes associated with the synthesis of precursors, namely UDP-glucose and UDP-*N*-acetylglucosamine, is a common strategy for improving the production of chondroitin and other glycosaminoglycans [3,7,56–58]. Interestingly, all the optimization

results obtained herein indicated genes that lead to UDP-*N*-acetylglucosamine production, suggesting this intermediate as the limiting precursor in *S. cerevisiae*.

Regarding the flux variability analysis (FVA), the difference between the predicted minimum and maximum chondroitin production shows that mutants are moderately robust.

In MEWpy, the optimization using evolutionary algorithms resulted in 75 solutions that included modifications in 53 different genes. The frequency and expression values of genes resulting from optimization are shown in Figure 3.

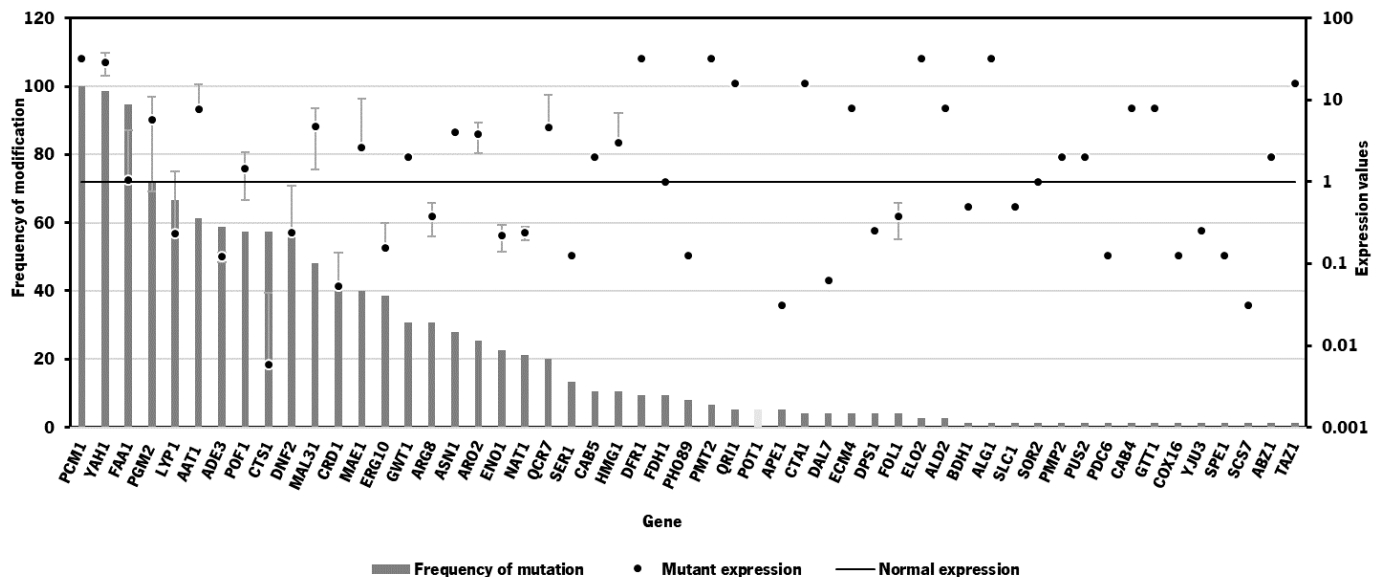


Figure 3. Frequency and expression values of genes in the solutions from optimization of *Saccharomyces cerevisiae* model for chondroitin production using MEWpy tool, limiting number of modifications to 10. The mutant expression (in dots) represents the average expression value. Mutant expressions higher than 1 represent overexpression while values of expression lower than 1 represent underexpression. Deletion is represented using a light grey bar. Gene descriptions: *AAT1*—mitochondrial aspartate aminotransferase; *ABZ1*—para-aminobenzoate synthase; *ADE3*—cytoplasmic trifunctional enzyme; *ALD2*—cytoplasmic aldehyde dehydrogenase; *ALG1*—mannosyltransferase; *APE1*—vacuolar aminopeptidase; *ARG8*—acetylornithine aminotransferase; *ASN1*—asparagine synthetase; *ARO2*—bifunctional chorismate synthase and flavin reductase; *BDH1*—NAD-dependent (R,R)-butanediol dehydrogenase; *CAB4/5*—subunits of the CoA-synthesizing protein complex; *COX16*—mitochondrial inner membrane protein; *CRD1*—cardiolipin synthase; *CTA1*—catalase A; *CTS1*—endochitinase; *DAL7*—malate synthase; *DFR1*—dihydrofolate reductase; *DNF2*—aminophospholipid translocase; *ECM4*—S-glutathionyl-(chloro)hydroquinone reductase; *DPS1*— aspartyl-tRNA synthetase; *ELO2*—fatty acid elongase; *ENO1*—enolase I; *ERG10*—acetyl-CoA C-acetyltransferase; *FAA1*—long chain fatty acyl-CoA synthetase; *FDH1*—NAD(+)-dependent formate dehydrogenase; *FOL1*—multifunctional enzyme of the folic acid biosynthesis pathway; *GTT1*—glutathione S-transferase; *GWT1*—phosphatidylinositol glycan anchored wall transfer protein; *HMG1*—3-hydroxy-3-methylglutaryl-CoA reductase; *LYP1*—lysine permease; *MAL31*—maltose permease; *MAE1*—mitochondrial malic enzyme; *NAT1*—subunit of protein N-terminal acetyltransferase; *PCM1*—N-acetylglucosamine-phosphate mutase; *PDC6*—minor isoform of pyruvate decarboxylase; *PGM2*—phosphoglucomutase; *PHO89*—plasma membrane Na⁺/Pi cotransporter; *PMP2*—proteolipid associated with plasma membrane H(+)-ATPase; *PMT2*—Protein O-mannosyltransferase; *POF1*—nicotinamide mononucleotide-specific adenylyltransferase; *POT1*—3-ketoacyl-CoA thiolase; *PUS2*—mitochondrial tRNA:pseudouridine synthase; *QCR7*—subunit 7 of ubiquinol cytochrome-c reductase; *QR11*—uridine diphosphate-*N*-acetylglucosamine pyrophosphorylase; *SCS7*—sphingolipid alpha-hydroxylase; *SER1*—3-phosphoserine aminotransferase; *SLC1*—1-acyl-sn-glycerol-3-phosphate acyltransferase; *SPE1*—ornithine decarboxylase; *SOR2*—sorbitol dehydrogenase; *TAZ1*—lyso-phosphatidylcholine acyltransferase; *YAH1*—ferredoxin of the mitochondrial matrix; *YJU3*—monoglyceride lipase.

All solutions presented one common modification, namely the overexpression of *PCMI*, a modification already identified by the OptFlux approach, which confirms it as a valuable strategy for improving chondroitin titers in engineered yeast cells. *QRI1* overexpression was also identified in the MEWpy approach, but only in four of the solutions. However, *GNA1* was not identified as a target in the MEWpy optimization. Instead, another gene (commonly signaled for overexpression) involved in the production of chondroitin precursors, *PGM2*, was identified by MEWpy as a potential target for optimization. This gene encodes phosphoglucomutase, appearing in 54 solutions (in the fourth place, Figure 3). As shown in Figure 2, this gene contributes to the production of UDP-glucose precursor.

The second most common modification found was the overexpression of *YAH1*, which encodes yeast adrenodoxin homolog, a ferredoxin involved in heme A biosynthesis by transferring electrons from nicotinamide adenine dinucleotide phosphate reduced form (NADPH) to heme O. The relationship between the overexpression of *YAH1* and the potential improvement of chondroitin production might not be immediately apparent. However, *YAH1* plays a crucial role in the electron transport chain and cellular redox balance within the mitochondria, and its overexpression leads to accumulation of heme A [59]. Consequently, the nicotinamide adenine dinucleotide oxidized form (NAD⁺) generated in this process could potentially be utilized in one of the reactions involved in chondroitin production, particularly the reaction catalyzed by UGD. This reaction requires NAD⁺ as a co-factor, converting it to nicotinamide adenine dinucleotide reduced form (NADH) during the transformation of UDP-glucose into UDP-glucuronic acid.

The third most frequently identified gene target was the long chain fatty acyl-CoA synthetase gene (*FAA1*), which was observed either as overexpression or underexpression, depending on the proposed solution. Due to the inconsistency in the recommended gene expression for this gene, it can be inferred that its contribution to the enhancement of chondroitin production might not be significant.

The solutions with higher BPCY are described in Table 3. Among the genes identified in the solutions with highest BPCY, only *QRI1* and *PCMI* were found to be directly involved in the pathways associated with chondroitin production (Figure 2).

Table 3. Optimization results obtained for *Saccharomyces cerevisiae* model using MEWpy tool, allowing for a maximum of 10 modifications. Growth rate and chondroitin production rate were predicted by phenotype simulations using parsimonious flux balance analysis (pFBA) and are presented in units of h⁻¹ and mmol/g_{DW}/h, respectively. BPCY was calculated by multiplying biomass growth rate by the flux of secreted product, and then dividing by the flux of consumed substrate. WYIELD is the weighted sum of the minimum and maximum product fluxes, with a default weight of 0.3 for maximum and 0.7 for minimum. Flux variability analysis (FVA) results are shown as minimum and maximum chondroitin obtained for fixed biomass.

| Solution | BPCY | WYIELD | Genes Modified | | | Predicted Phenotype (pFBA) | | FVA | |
|----------|---------|---------|-------------------------|-------------------------|--|----------------------------|--|--|--|
| | | | Knock-Out | Under Expression | Over Expression | Biomass (h ⁻¹) | Chondroitin Flux (mmol/g _{DW} /h) | Minimum Chondroitin Flux (mmol/g _{DW} /h) | Maximum Chondroitin Flux (mmol/g _{DW} /h) |
| 1 | 0.04375 | 0.60872 | <i>DNF2, CTS1</i> | <i>CRD1, LYP1, FAA1</i> | <i>YAH1, QRI1, PCMI, CAB5</i> | 0.7317 | 0.5980 | 0.5980 | 0.9358 |
| 2 | 0.04374 | 0.60872 | <i>FAA1, POT1, CTS1</i> | <i>MAL31, ARG8</i> | <i>YAH1, PCMI, ALD2</i> | 0.7316 | 0.5980 | 0.5980 | 0.9358 |
| 3 | 0.04335 | 0.60876 | <i>ENO1, CTS1</i> | <i>ERG10</i> | <i>FAA1, YAH1, AAT1, POF1, CTA1, PCMI, MAL31</i> | 0.7248 | 0.5981 | 0.5981 | 0.9365 |

Gene descriptions: *AAT1*—aspartate aminotransferase; *ALD2*—aldehyde dehydrogenase; *ARG8*—acetylornithine aminotransferase; *CAB5*—subunit of the CoA-Synthetizing Protein Complex; *CRD1*—cardiolipin synthase; *CTA1*—catalase A; *CTS1*—endochitinase; *DNF2*—phospholipid-transporting ATPase; *ENO1*—enolase I; *ERG10*—acetyl-CoA C-acetyltransferase; *FAA1*—long chain fatty acyl-CoA synthetase; *LYP1*—lysine permease; *MAL31*—maltose permease; *PCMI*—N-acetylglucosamine-phosphate mutase; *POF1*—nicotinamide mononucleotide-specific adenylyltransferase; *POT1*—3-ketoacyl-CoA thiolase; *QRI1*—UDP-N-acetylglucosamine pyrophosphorylase; *YAH1*—yeast adrenodoxin homolog.

However, there are several indirect relationships where modifications to other gene expressions may impact the in silico chondroitin production. For instance, the overexpression of the gene *POF1*, which encodes nicotinamide mononucleotide-specific adenylyltransferase, catalyzes the conversion of nicotinamide mononucleotide to NAD^+ , an essential co-factor in chondroitin production, as discussed earlier. Therefore, the identification of *POF1* overexpression may be related with the attempt to improve NAD^+ pool. Additionally, *CTS1*, which encodes endochitinase, was identified as a knockout target. As observed in Figure 2, chitin formation competes with chondroitin production pathway for UDP-acetylglucosamine substrate. Knocking out *CTS1* could redirect cellular resources and energy, that would have been used for chitin breakdown, towards the biosynthesis of chondroitin. This redirection could enhance the overall yield and efficiency of chondroitin production.

The size of the resulting solutions was between 8 and 10 genetic modifications. However, the BPCY was not higher than the one obtained in the OptFlux solutions, where only one gene expression was altered. In terms of FVA analysis, the robustness from MEWpy solutions was neither higher nor lower than the ones from OptFlux approach. Also, changing the gene expression of 8 to 10 genes would be difficult to implement and would possibly significantly affect the *S. cerevisiae* growth. Therefore, the optimization was again run, now limiting the number of modifications to three. The new optimization using MEWpy led to 28 solutions. These solutions included modifications in 14 different genes. The frequency and expression value of each gene throughout the solutions is presented in Figure 4.

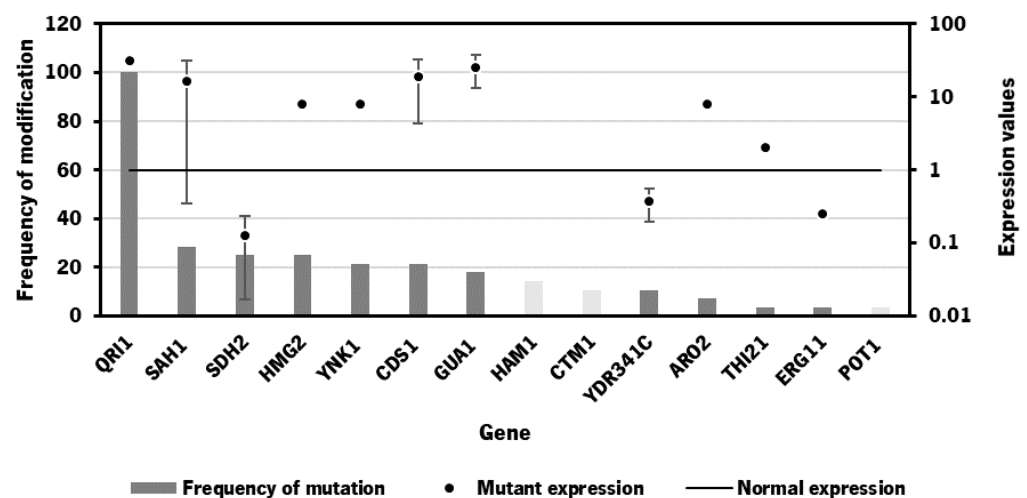


Figure 4. Frequency and expression values of genes in the solutions from optimization of *Saccharomyces cerevisiae* model using MEWpy tool, limiting number of modifications to 3. The mutant expression (in dots) represents the average expression value. Mutant gene expression values higher than 1 represent overexpression, while values of expression lower than 1 represent underexpression. Deletions are represented in light grey bars. Gene descriptions: *ARO2*—bifunctional chorismate synthase and flavin reductase; *CDS1*—phosphatidate cytidyltransferase; *CTM1*—cytochrome c lysine methyltransferase; *ERG11*—lanosterol 14- α -demethylase; *GUA1*—guanosine monophosphate synthase; *HAM1*—nucleoside triphosphate pyrophosphohydrolase; *HMG2*—3-hydroxy-3-methylglutaryl-CoA reductase; *POT1*—3-ketoacyl-CoA thiolase; *QRI1*—uridine diphosphate-*N*-acetylglucosamine pyrophosphorylase; *SAH1*—*S*-adenosyl-*L*-homocysteine hydrolase; *SDH2*—iron-sulfur protein subunit of succinate dehydrogenase; *THI21*—hydroxymethylpyrimidine (HMP) and HMP-phosphate kinase; *YDR341C*—arginyl-tRNA synthetase; *YNK1*—nucleoside diphosphate kinase.

In this case, all solutions included *QRI1* overexpression, which was also predicted in the above-mentioned approaches (Table 2 and Figure 3). The best solutions in terms of BPCY are described in Table 4.

Table 4. Optimization results obtained for *Saccharomyces cerevisiae* model using MEWpy tool, allowing for a maximum of 3 modifications. Growth rate and chondroitin production rate were predicted by phenotype simulations using parsimonious flux balance analysis (pFBA) and are presented in units of h^{-1} and $\text{mmol/g}_{\text{DW}}/\text{h}$, respectively. BPCY was calculated by multiplying biomass growth rate by the flux of secreted product and then dividing by the flux of consumed substrate. WYIELD is the weighted sum of the minimum and maximum product fluxes, with a default weight of 0.3 for maximum and 0.7 for minimum. Flux variability analysis (FVA) results are shown as minimum and maximum chondroitin obtained for fixed biomass.

| Solution | BPCY | WYIELD | Genes Modified | | | Predicted Phenotype (pFBA) | | FVA | |
|----------|---------|---------|----------------|------------------|-----------------|-----------------------------|---|---|---|
| | | | Knock-Out | Under Expression | Over Expression | Biomass (h^{-1}) | Chondroitin Flux ($\text{mmol/g}_{\text{DW}}/\text{h}$) | Minimum Chondroitin Flux ($\text{mmol/g}_{\text{DW}}/\text{h}$) | Maximum Chondroitin Flux ($\text{mmol/g}_{\text{DW}}/\text{h}$) |
| 1 | 0.04375 | 0.83445 | - | - | <i>QR11</i> | 0.7317 | 0.5980 | 0.5980 | 0.9358 |
| 2 | 0.01488 | 2.80306 | <i>CTM1</i> | <i>CDS1</i> | <i>QR11</i> | 0.0541 | 0.6131 | 0.6131 | 3.7416 |
| 3 | 0.04359 | 0.83489 | <i>HAM1</i> | <i>SDH2</i> | <i>QR11</i> | 0.7288 | 0.5980 | 0.5980 | 0.9364 |

Gene descriptions: *CDS1*—phosphatidate cytidyltransferase; *CTM1*—cytochrome c lysine methyltransferase; *HAM1*—Nucleoside triphosphate pyrophosphohydrolase; *QR11*—uridine diphosphate-*N*-acetylglucosamine pyrophosphorylase; *SDH2*—iron-sulfur protein subunit of succinate dehydrogenase.

For future work, other types of models should be explored for more meaningful results on the identification of targets for metabolic engineering. While GEMs can give insights into novel metabolic engineering targets, the phenotype prediction could be more accurate if kinetic data, enzyme usage-constraints and regulatory information were included in the model. For example, GECKO is a method that enhances a GEM to account for enzymes as part of reactions and has been applied to a *S. cerevisiae* model [60]. Nevertheless, in the future, genetic modifications such as *QR11*, *GNA1*, and/or *PCM1* overexpression, should be tested to improve chondroitin production in *S. cerevisiae*, as suggested by the results obtained herein.

3. Materials and Methods

3.1. Strains and Plasmids

The strains and plasmids used in this study are listed in Table 5. *E. coli* NZY5 α (NZYTech, Lisbon, Portugal) competent cells were used for cloning procedures, vector propagation, and storage. *E. coli* was cultured at 37 °C and 200 rpm in lysogeny broth (LB) (10 g/L tryptone, 5 g/L yeast extract, 10 g/L NaCl; NZYTech) or on LB agar plates (20 g/L agar, JMGS, Odivelas, Portugal). Ampicillin (NZYTech) at a final concentration of 100 $\mu\text{g}/\text{mL}$ was supplemented when necessary.

S. cerevisiae CEN.PK2-1C and *S. cerevisiae* BY4741 strains were obtained from Euroscarf (Oberursel, Germany). The plasmids pSP-GM1 (PGK1 promoter and TEF promoter; Adgene, Watertown, MA, USA) and pBEVY-L (GPD promoter; ATCC, Manassas, USA) were used as shuttle vectors. Wild-type yeast strains were cultivated at 30 °C and 200 rpm in yeast extract peptone dextrose (YPD) media, composed by 20 g/L bacteriological peptone (HiMedia, Mumbai, India), 10 g/L yeast extract (Panreac AppliChem, Darmstadt, Germany), 20 g/L glucose (Acros Organics, Branchburg, NJ, USA), or in agar plates with the same composition.

The engineered yeast strains were grown in synthetic defined minimal media composed of 6.7 g/L of yeast nitrogen base (YNB) with ammonium sulfate without amino acids (Sigma Aldrich, Steinheim, Germany), supplemented with 20 g/L glucose and the required amino acids to compensate for auxotrophies, namely tryptophan or methionine (Panreac AppliChem), depending on the strain, and histidine (Panreac AppliChem) at final concentrations of 100 mg/L.

Table 5. Strains and plasmids used in this study.

| Strains | Relevant Genotype | Source |
|--|--|-----------------------|
| <i>Escherichia coli</i> NZY5 α | <i>fnuA2</i> Δ (<i>argF-lacZ</i>)U169 <i>phoA glnV44</i> Φ 80 Δ (<i>lacZ</i>)M15 <i>gyrA96 recA1 relA1 endA1 thi-1 hsdR17</i> | NZYTech (MB00401) |
| <i>Saccharomyces cerevisiae</i> CEN.PK2-1C | MATa <i>ura3-52 his3</i> Δ 1 <i>leu2-3,112 trp1-289 MAL2-8^c</i> SUC2 | Euroscarf 30000A [61] |
| <i>S. cerevisiae</i> BY4741 | MATa <i>his3</i> Δ 1 <i>leu2</i> Δ 0 <i>met15</i> Δ 0 <i>ura3</i> Δ 0 | Euroscarf Y00000 [62] |
| Plasmids | Description | Source |
| pSP-GM1 | pUC <i>ori</i> , Amp ^R , 2 μ <i>ori</i> , URA3 P _{TEF1} P _{PGK1} | Addgene #64739 [63] |
| pBEVY-L | pUC <i>ori</i> , Amp ^R , 2 μ <i>ori</i> , LEU2 P _{GPD} P _{ADHI} | ATCC 51226 |
| pUC57_Giuae | pMB1 <i>ori</i> , Amp ^R ; pUC57 carrying <i>Giardia intestinalis</i> uridine diphosphate-glucosamine-4-epimerase gene (<i>GiUAE</i>) codon-optimized for <i>S. cerevisiae</i> | NZYTech |
| pUC57_Btchsy1 | pMB1 <i>ori</i> , Amp ^R ; pUC57 carrying <i>Bos taurus</i> chondroitin synthase 1 gene (<i>BtCHSY</i>) codon-optimized for <i>S. cerevisiae</i> | NZYTech |
| pETM6_kfoCA | pETM6 carrying chondroitin synthase, <i>kfoC</i> , and, uridine diphosphate-glucosamine-4-epimerase, <i>kfoA</i> , genes from <i>E. coli</i> O5:K4:H4 | [5] |
| pSP-GM1_Zmugd | pSP-GM1 carrying <i>Zymomonas mobilis</i> uridine diphosphate glucose 6-dehydrogenase gene (<i>Zmugd</i>) | [46] |
| pSP-GM1_Giuae_Zmugd | pSP-GM1 carrying <i>GiUAE</i> and <i>Zmugd</i> | This study |
| pBEVY_Btchsy | pBEVY-L carrying <i>BtCHSY</i> | This study |
| pSP-GM1_kfoA_Zmugd | pSP-GM1 carrying <i>kfoA</i> and <i>Zmugd</i> | This study |
| pBEVY_kfoC | pBEVY-L carrying <i>kfoC</i> | This study |

3.2. Biosynthetic Pathway Construction

Table S1 compiles the primers used for cloning procedures. Two different biosynthetic pathways were constructed and introduced in *S. cerevisiae* CEN.PK2-1C and *S. cerevisiae* BY4741 strains. Each pathway contained three genes for the expression of UGD, UAE, and CHSY, which are absent in yeast metabolism. *GiUAE* (GenBank accession number AY187036.1) and *BtCHSY* (GenBank accession number AF440749.1) were codon-optimized for *S. cerevisiae* and synthesized by NZYTech (sequences are presented in Table S2). Afterwards, *GiUAE* and *BtCHSY* were amplified from pUC57_Giuae and pUC57_Btchsy, respectively, using Gi_uae_Fw1 and Gi_uae_Rv1 or Bt_chsy1_Fw and Bt_chsy1_Rv as primers. After amplification, genes were first independently cloned in pSP-GM1 under PGK1 promoter. For further assembly of the entire chondroitin pathway, the *GiUAE* was cloned in pSP-GM1 under the TEF promoter regulation, using the primers Giuae_tefp_Fw and Giuae_tefp_Rv for gene amplification. Then, *Zmugd*, amplified from pSP-GM1_Zmugd [46] with primers Zm_psp_Fw and Zm_psp_Rv, was cloned in pSP-GM1_Giuae_tef, resulting in pSP-GM1_Giuae_Zmugd (*Zmugd* was cloned second as the restriction enzymes used to clone *GiUAE* cut *Zmugd*, that is not codon-optimized). The *BtCHSY* was amplified from pSP-GM1_Btchsy, using the primers Btchsy_pBEVY_Fw and Btchsy_pBEVY_Rv, and cloned in pBEVY-L generating pBEVY_Btchsy. The second pathway was composed of chondroitin-producing genes *kfoA* and *kfoC* (encoding UAE and CHSY, respectively) from *E. coli* K4 (serotype O5:K4(L):H4). *KfoA* and *kfoC* were amplified from pETM6_kfoCA [5], which was kindly provided by Dr. Mattheos Kofas (Rensselaer Polytechnic Institute, Troy, NY, USA). For that purpose, the primer pairs *kfoA_psp_Fw/kfoA_psp_Rv* and *kfoC_pBEVY_Fw/kfoC_pBEVY_Rv* were used, respectively. Then, *kfoA* was cloned into pSP-GM1_Zmugd [46] while *kfoC* was cloned in pBEVY-L, resulting in pSP-GM1_kfoA_Zmugd and pBEVY_kfoC, respectively.

All gene amplifications were performed through PCR (polymerase chain reaction) using Phusion High Fidelity DNA Polymerase (Thermo Fisher Scientific, Wilmington, NC, USA). The plasmids were extracted with Plasmid Miniprep Kit (Macherey-Nagel, Düren, Germany). PCR products were excised and purified from agarose gels using NucleoSpin[®] Gel and PCR Clean-up Kit (Macherey-Nagel). Quantification of plasmid DNA and PCR products was further achieved using NanoDrop One instrument (Thermo Fisher Scientific). Then, digestion was performed by incubating specific restriction endonucleases (Thermo Fisher Scientific) for 1 h at 37 °C. The resulting digested DNA fragments were purified using NucleoSpin[®] Gel and PCR Clean-up Kit and used for ligations with T4 DNA ligase (Thermo Fisher Scientific) for 1 h at room temperature. The resulting mixture was transformed into *E. coli* NZY5 α competent cells (NZYTech) by heat shock. Transformants were then recovered by adding super optimal broth with catabolite repression (SOC; NZYTech) and incubating the mixture for 1 h at 37 °C. Cells were then plated on agar plates containing selective medium. Finally, all construction sequences were verified by colony PCR using Dream Taq polymerase (Thermo Fisher Scientific), digestion, and further confirmation by sequencing (GATC Biotech, Konstanz, Germany). After sequence confirmation, transformations of the constructed plasmids into *S. cerevisiae* were performed by the lithium acetate/single-stranded carrier DNA/polyethylene glycol method [64]. Lithium acetate, salmon sperm DNA, and polyethylene glycol (PEG-3350) were obtained from Sigma-Aldrich. Selection of yeast transformants was performed in synthetic defined minimal media with the required amino acids.

3.3. Flask Fermentation Conditions

For each assay, a single *S. cerevisiae* colony was picked from the transformation plate and grown for 24 h at 30 °C and 200 rpm in 8 mL of the synthetic defined minimal media supplemented with the required amino acids for pre-culture. Afterwards, 50 mL of medium with the same composition in 250 mL flasks was inoculated to an initial optical density at 600 nm (OD_{600nm}) of 0.1. Yeast cells were further cultured at 30 °C and 200 rpm for 24 h.

3.4. Analytical Methods

At the end of the fermentation, the culture of *S. cerevisiae* cells (~50 mL) was harvested by centrifugation (5000 \times g, 15 min). The supernatants were used to quantify extracellular chondroitin and glucose, while the pellets were further processed to determine intracellular chondroitin.

To obtain the intracellular fraction, cells were lysed. For each 0.1 g of wet cells, 0.2 g of glass beads (425–600 μ m, Sigma-Aldrich) was added to the cell pellet, as well as 1 mL of deionized water. The cells were then lysed in FastPrep-24 (MP Biomedicals, Salon, OH, USA) during 5 cycles of 1 min at 6–6.5 m/s, interspersed with 1 min cooling on ice. The lysed samples were centrifuged (16,000 \times g, 15 min). Afterwards, the lysates (supernatant) were treated with DNaseI (New England Biolabs, MA, USA) for 2 h at 37 °C, followed by treatment with proteinase K (2 mg/mL, NZYTech) for 2 h at 56 °C. The mixture was further boiled for 5 min and centrifuged (16,000 \times g, 20 min) to remove insoluble material.

To precipitate extracellular and intracellular chondroitin, three volumes of cold ethanol were added to the samples, and the mixture was left at 4 °C overnight. The resulting precipitate was collected through centrifugation (4000 \times g for 10 min at 4 °C) and subsequently air-dried at room temperature overnight. The dried precipitate was resuspended in deionized water, followed by removal of the insoluble material by centrifugation (16,000 \times g, 20 min). Uronic acid carbazole assay [65] was used to estimate chondroitin production by using chondroitin sulfate (Biosynth, Staad, Switzerland) solutions as standards. Standards or samples with 125 μ L were mixed with 750 μ L sulfuric acid reagent (9.5 g/L sodium tetraborate, Supelco, Bellefonte, USA, dissolved in H₂SO₄ > 95%, Fisher Chemical, Hampton, VA, USA) and boiled for 20 min. Then, 25 μ L of carbazole reagent (1.25 g/L carbazole, Supelco, dissolved in absolute ethanol, Fisher Chemical) was added to the boiled samples, followed by an additional 15 min of boiling and a subsequent 15 min of cooling.

The OD_{530nm} was measured using a 96-well plate spectrophotometric reader Synergy HT (BioTek, Winooski, VT, USA).

Yeast cell concentration was calculated by determining the OD_{600nm} at the end of culture, using a calibration with solutions of known biomass concentration.

Glucose samples at the end of fermentation were analyzed using high performance liquid chromatography (HPLC) with a JASCO system and a refractive index (RI) detector (RI-2031), employing an Aminex HPX-87H column from Bio-Rad maintained at 60 °C. The mobile phase used was 5 mM H₂SO₄ at a flow rate of 0.5 mL/min.

3.5. Model Construction

The consensus GEM of *Saccharomyces cerevisiae* yeast-GEM [66], version 8.4.2 (<https://github.com/SysBioChalmers/yeast-GEM>, accessed on 25 March 2023), composed of 4058 reactions, 2742 metabolites, and 1150 genes, was used as a template. From this, a new model containing the heterologous pathway for chondroitin production was constructed by including the reactions UGD, UAE, and CHSY. The metabolites UDP-glucose (S_1543) and UDP-acetylglucosamine (S_1544) were already available in the template model. UDP-glucuronic acid (M_udpglcur), UDP-acetylgalactosamine (M_udpacgal), and chondroitin (M_chond) were included. The genes for the reactions UGD, UAE, and CHSY were also added to the model. After preliminary tests, the biomass equation was adjusted to include 1% chitin in the biomass composition. The final model, labelled yeast-GEM_c, included 4062 reactions, 2745 metabolites, and 1153 genes.

3.6. Conditions for In Silico Simulations and Optimization

The OptFlux software [67] (version 3.3.5) was used to simulate the phenotype of *S. cerevisiae* engineered with chondroitin production pathway and further mutants, using parsimonious flux balance analysis (pFBA) as the simulation method [68]. Glucose uptake was set to 10 mmol/g_{DW}/h, and oxygen was unrestricted (1000 mmol/g_{DW}/h). The identification of gene deletion and over/under expression targets to optimize chondroitin production was performed by running optimization algorithms. The Strength Pareto Evolutionary Algorithm 2 (SPEA2) [69] was used as optimization strategy, with the BPCY set as the objective, and pFBA as the simulation method. pFBA used the biomass reaction (r_2111) as the objective function to maximize. A maximum of 10 modifications were allowed. The maximum for evaluation functions was set to 50,000. CPLEX Optimization Studio version 12.9.0 (IBM) was used as linear programming solver.

The identification of chondroitin optimization targets was also performed using MEWpy [70] (the XML file is available in Supplementary File 2) under the same environmental conditions as before, using the Evolutionary Algorithm Non-Dominated Sorting Genetic Algorithm II [71] as optimization strategy and pFBA as the simulation method. The evolutionary algorithm employed two objective functions, BPCY and weighted yield (WYIELD, weighed sum of the minimum and maximum product fluxes). pFBA used the biomass reaction as the objective function to maximize. A maximum of 10 or 3 modifications were allowed.

FVA of chondroitin production [72] was performed to assess the robustness of the optimization results.

4. Conclusions

Chondroitin stands as a valuable natural compound with a wide range of practical uses in the health sector. Its biotechnological production presents an intriguing opportunity. As *S. cerevisiae* is a robust, fast-growing, and easily mutated host, it was selected to be engineered with chondroitin biosynthetic pathways. Also, this is an alternative host that should be considered for chondroitin production due to its ability to perform post-translational modifications. In this study, novel biosynthetic pathways were evaluated for producing chondroitin in *S. cerevisiae*, and up to 125 mg/L and 200 mg/L of extracellular and intracellular chondroitin, respectively, were obtained through flask fermentation. Since

the application of computational-aided metabolic engineering might help discover critical bottlenecks in *S. cerevisiae* heterologous biosynthesis, a metabolic model and flux analysis were also used herein for strain design. The model yeast-GEM_c was constructed using yeast GEM as scaffold in which chondroitin production reactions and genes were included. Using evolutionary algorithms, several promising novel targets, such as *QR11*, *GNA1*, or *PCM1* overexpression, were identified as promising to improve chondroitin titers of engineered *S. cerevisiae* strains. The use of the evaluated pathways to construct the predicted in silico engineered strains, in combination with other methods, such as integration of genes in the yeast genome, can lead to further improved chondroitin yields. Concluding, this study demonstrated the successful production of chondroitin for the first time and the strategy reported herein can serve as a basis for developing industrial *S. cerevisiae* strains capable of efficient chondroitin production.

Supplementary Materials: The following supporting information can be downloaded at: <https://www.mdpi.com/article/10.3390/synbio2020008/s1>. Supplementary file 1: Table S1: Primers used in this study; Table S2. Codon-optimized gene sequences (5' → 3') for *Saccharomyces cerevisiae*. Supplementary file 2: *S. cerevisiae* model file.

Author Contributions: M.R.C. performed the experiments, analyzed the data and drafted the manuscript. O.D. conducted MEWpy experiments on Python. J.L.R. and L.R.R. supervised and coordinated the study and provided feedback and suggestions on the manuscript. L.R.R. provided funds for the research development. All authors have read and agreed to the published version of the manuscript.

Funding: This study was supported by the Portuguese Foundation for Science and Technology (FCT) under the scope of the strategic funding of UIDB/04469/2020 unit with DOI 10.54499/UIDB/04469/2020. The authors acknowledge FCT for funding MRC doctoral grant SFRH/BD/132998/2017 and further extension COVID/BD/152454/2022.

Institutional Review Board Statement: Not applicable.

Informed Consent Statement: Not applicable.

Data Availability Statement: Dataset available on request from the authors.

Conflicts of Interest: The authors declare no conflict of interest. The funders had no role in the design of the study; in the collection, analyses, or interpretation of data; in the writing of the manuscript; or in the decision to publish the results.

References

1. Couto, M.R.; Rodrigues, J.L.; Rodrigues, L.R. Heterologous production of chondroitin. *Biotechnol. Rep.* **2022**, *33*, e00710. [[CrossRef](#)]
2. Cress, B.F.; Englaender, J.A.; He, W.; Kasper, D.; Linhardt, R.J.; Koffas, M.A.G. Masquerading microbial pathogens: Capsular polysaccharides mimic host-tissue molecules. *FEMS Microbiol. Rev.* **2014**, *38*, 660–697. [[CrossRef](#)] [[PubMed](#)]
3. Cimini, D.; Carlino, E.; Giovane, A.; Argenzio, O.; Dello Iacono, I.; De Rosa, M.; Schiraldi, C. Engineering a branch of the UDP-precursor biosynthesis pathway enhances the production of capsular polysaccharide in *Escherichia coli* O5:K4:H4. *Biotechnol. J.* **2015**, *10*, 1307–1315. [[CrossRef](#)] [[PubMed](#)]
4. Jin, P.; Zhang, L.; Yuan, P.; Kang, Z.; Du, G.; Chen, J. Efficient biosynthesis of polysaccharides chondroitin and heparosan by metabolically engineered *Bacillus subtilis*. *Carbohydr. Polym.* **2016**, *140*, 424–432. [[CrossRef](#)] [[PubMed](#)]
5. He, W.; Fu, L.; Li, G.; Andrew Jones, J.; Linhardt, R.J.; Koffas, M.; Jones, J.A.; Linhardt, R.J.; Koffas, M.; Andrew Jones, J.; et al. Production of chondroitin in metabolically engineered *E. coli*. *Metab. Eng.* **2015**, *27*, 92–100. [[CrossRef](#)] [[PubMed](#)]
6. Cheng, F.; Luozhong, S.; Yu, H.; Guo, Z. Biosynthesis of Chondroitin in Engineered *Corynebacterium glutamicum*. *J. Microbiol. Biotechnol.* **2019**, *29*, 392–400. [[CrossRef](#)] [[PubMed](#)]
7. Zhou, Z.; Li, Q.; Huang, H.; Wang, H.; Wang, Y.; Du, G.; Chen, J.; Kang, Z. A microbial-enzymatic strategy for producing chondroitin sulfate glycosaminoglycans. *Biotechnol. Bioeng.* **2018**, *115*, 1561–1570. [[CrossRef](#)] [[PubMed](#)]
8. Jin, X.; Zhang, W.; Wang, Y.; Sheng, J.; Xu, R.; Li, J.; Du, G.; Kang, Z. Biosynthesis of non-animal chondroitin sulfate from methanol using genetically engineered *Pichia pastoris*. *Green Chem.* **2021**, *23*, 4365–4374. [[CrossRef](#)]
9. Desko, M.M.; Gross, D.A.; Kohler, J.J. Effects of N-glycosylation on the activity and localization of GlcNAc-6-sulfotransferase 1. *Glycobiology* **2009**, *19*, 1068–1077. [[CrossRef](#)]
10. Badri, A.; Williams, A.; Awofiranye, A.; Datta, P.; Xia, K.; He, W.; Fraser, K.; Dordick, J.S.; Linhardt, R.J.; Koffas, M.A.G.G. Complete biosynthesis of a sulfated chondroitin in *Escherichia coli*. *Nat. Commun.* **2021**, *12*, 1389. [[CrossRef](#)] [[PubMed](#)]

11. Nielsen, J. Yeast Systems Biology: Model Organism and Cell Factory. *Biotechnol. J.* **2019**, *14*, 1800421. [[CrossRef](#)] [[PubMed](#)]
12. Li, M.; Borodina, I. Application of synthetic biology for production of chemicals in yeast *Saccharomyces cerevisiae*. *FEMS Yeast Res.* **2015**, *15*, 1–12. [[CrossRef](#)] [[PubMed](#)]
13. Gupta, S.K.; Shukla, P. Sophisticated cloning, fermentation, and purification technologies for an enhanced therapeutic protein production: A review. *Front. Pharmacol.* **2017**, *8*, 419. [[CrossRef](#)] [[PubMed](#)]
14. Lopes, H.; Rocha, I. Genome-scale modeling of yeast: Chronology, applications and critical perspectives. *FEMS Yeast Res.* **2017**, *17*, fox050. [[CrossRef](#)] [[PubMed](#)]
15. Vieira, V.; Maia, P.; Rocha, M.; Rocha, I. Comparison of pathway analysis and constraint-based methods for cell factory design. *BMC Bioinform.* **2019**, *20*, 350. [[CrossRef](#)] [[PubMed](#)]
16. Maia, P.; Rocha, M.; Rocha, I. In Silico Constraint-Based Strain Optimization Methods: The Quest for Optimal Cell Factories. *Microbiol. Mol. Biol. Rev.* **2016**, *80*, 45–67. [[CrossRef](#)]
17. Bi, X.; Liu, Y.; Li, J.; Du, G.; Lv, X.; Liu, L. Construction of Multiscale Genome-Scale Metabolic Models: Frameworks and Challenges. *Biomolecules* **2022**, *12*, 721. [[CrossRef](#)]
18. Ng, R.H.; Lee, J.W.; Baloni, P.; Diener, C.; Heath, J.R.; Su, Y. Constraint-Based Reconstruction and Analyses of Metabolic Models: Open-Source Python Tools and Applications to Cancer. *Front. Oncol.* **2022**, *12*, 914594. [[CrossRef](#)] [[PubMed](#)]
19. Mardinoglu, A.; Nielsen, J. Systems medicine and metabolic modelling. *J. Intern. Med.* **2012**, *271*, 142–154. [[CrossRef](#)] [[PubMed](#)]
20. Zhang, C.; Hua, Q. Applications of genome-scale metabolic models in biotechnology and systems medicine. *Front. Physiol.* **2016**, *6*, 413. [[CrossRef](#)] [[PubMed](#)]
21. Fang, X.; Lloyd, C.J.; Palsson, B.O. Reconstructing organisms in silico: Genome-scale models and their emerging applications. *Nat. Rev. Microbiol.* **2020**, *18*, 731–743. [[CrossRef](#)] [[PubMed](#)]
22. Gu, C.; Kim, G.B.; Kim, W.J.; Kim, H.U.; Lee, S.Y. Current status and applications of genome-scale metabolic models. *Genome Biol.* **2019**, *20*, 121. [[CrossRef](#)] [[PubMed](#)]
23. Chen, X.; Xu, G.; Xu, N.; Zou, W.; Zhu, P.; Liu, L.; Chen, J. Metabolic engineering of *Torulopsis glabrata* for malate production. *Metab. Eng.* **2013**, *19*, 10–16. [[CrossRef](#)] [[PubMed](#)]
24. Xu, G.; Zou, W.; Chen, X.; Xu, N.; Liu, L.; Chen, J. Fumaric Acid Production in *Saccharomyces cerevisiae* by In Silico Aided Metabolic Engineering. *PLoS ONE* **2012**, *7*, 1–10. [[CrossRef](#)] [[PubMed](#)]
25. Otero, J.M.; Cimini, D.; Patil, K.R.; Poulsen, S.G.; Olsson, L.; Nielsen, J. Industrial Systems Biology of *Saccharomyces cerevisiae* Enables Novel Succinic Acid Cell Factory. *PLoS ONE* **2013**, *8*, 1–10. [[CrossRef](#)] [[PubMed](#)]
26. Song, C.W.; Kim, D.I.; Choi, S.; Jang, J.W.; Lee, S.Y. Metabolic engineering of *Escherichia coli* for the production of fumaric acid. *Biotechnol. Bioeng.* **2013**, *110*, 2025–2034. [[CrossRef](#)] [[PubMed](#)]
27. Chen, X.; Wu, J.; Song, W.; Zhang, L.; Wang, H.; Liu, L. Fumaric acid production by *Torulopsis glabrata*: Engineering the urea cycle and the purine nucleotide cycle. *Biotechnol. Bioeng.* **2015**, *112*, 156–167. [[CrossRef](#)] [[PubMed](#)]
28. Harder, B.J.; Bettenbrock, K.; Klamt, S. Model-based metabolic engineering enables high yield itaconic acid production by *Escherichia coli*. *Metab. Eng.* **2016**, *38*, 29–37. [[CrossRef](#)]
29. Mishra, P.; Lee, N.-R.; Lakshmanan, M.; Kim, M.; Kim, B.-G.; Lee, D.-Y. Genome-scale model-driven strain design for dicarboxylic acid production in *Yarrowia lipolytica*. *BMC Syst. Biol.* **2018**, *12*, 12. [[CrossRef](#)] [[PubMed](#)]
30. Bro, C.; Regenberg, B.; Förster, J.; Nielsen, J. In silico aided metabolic engineering of *Saccharomyces cerevisiae* for improved bioethanol production. *Metab. Eng.* **2006**, *8*, 102–111. [[CrossRef](#)] [[PubMed](#)]
31. Yim, H.; Haselbeck, R.; Niu, W.; Pujol-Baxley, C.; Burgard, A.; Boldt, J.; Khandurina, J.; Trawick, J.D.; Osterhout, R.E.; Stephen, R.; et al. Metabolic engineering of *Escherichia coli* for direct production of 1,4-butanediol. *Nat. Chem. Biol.* **2011**, *7*, 445–452. [[CrossRef](#)] [[PubMed](#)]
32. Ng, C.; Jung, M.; Lee, J.; Oh, M.-K. Production of 2,3-butanediol in *Saccharomyces cerevisiae* by in silico aided metabolic engineering. *Microb. Cell Factories* **2012**, *11*, 68. [[CrossRef](#)] [[PubMed](#)]
33. Becker, J.; Zelder, O.; Häfner, S.; Schröder, H.; Wittmann, C. From zero to hero-Design-based systems metabolic engineering of *Corynebacterium glutamicum* for l-lysine production. *Metab. Eng.* **2011**, *13*, 159–168. [[CrossRef](#)] [[PubMed](#)]
34. Park, J.H.; Kim, T.Y.; Lee, K.H.; Lee, S.Y. Fed-batch culture of *Escherichia coli* for L-valine production based on in silico flux response analysis. *Biotechnol. Bioeng.* **2011**, *108*, 934–946. [[CrossRef](#)] [[PubMed](#)]
35. van Ooyen, J.; Noack, S.; Bott, M.; Reth, A.; Eggeling, L. Improved L-lysine production with *Corynebacterium glutamicum* and systemic insight into citrate synthase flux and activity. *Biotechnol. Bioeng.* **2012**, *109*, 2070–2081. [[CrossRef](#)] [[PubMed](#)]
36. Jung, Y.K.; Kim, T.Y.; Park, S.J.; Lee, S.Y. Metabolic engineering of *Escherichia coli* for the production of polylactic acid and its copolymers. *Biotechnol. Bioeng.* **2010**, *105*, 161–171. [[CrossRef](#)] [[PubMed](#)]
37. Poblete-Castro, I.; Binger, D.; Rodrigues, A.; Becker, J.; Martins Dos Santos, V.A.P.; Wittmann, C. In-silico-driven metabolic engineering of *Pseudomonas putida* for enhanced production of poly-hydroxyalkanoates. *Metab. Eng.* **2013**, *15*, 113–123. [[CrossRef](#)] [[PubMed](#)]
38. Kildegaard, K.R.; Jensen, N.B.; Schneider, K.; Czarnotta, E.; Özdemir, E.; Klein, T.; Maury, J.; Ebert, B.E.; Christensen, H.B.; Chen, Y.; et al. Engineering and systems-level analysis of *Saccharomyces cerevisiae* for production of 3-hydroxypropionic acid via malonyl-CoA reductase-dependent pathway. *Microb. Cell Factories* **2016**, *15*, 53. [[CrossRef](#)] [[PubMed](#)]
39. Yang, J.E.; Park, S.J.; Kim, W.J.; Kim, H.J.; Kim, B.J.; Lee, H.; Shin, J.; Lee, S.Y. One-step fermentative production of aromatic polyesters from glucose by metabolically engineered *Escherichia coli* strains. *Nat. Commun.* **2018**, *9*, 79. [[CrossRef](#)] [[PubMed](#)]

40. Kim, M.; Sang Yi, J.; Kim, J.; Kim, J.N.; Kim, M.W.; Kim, B.G. Reconstruction of a high-quality metabolic model enables the identification of gene overexpression targets for enhanced antibiotic production in *Streptomyces coelicolor* A3(2). *Biotechnol. J.* **2014**, *9*, 1185–1194. [[CrossRef](#)] [[PubMed](#)]
41. Huang, D.; Wen, J.; Wang, G.; Yu, G.; Jia, X.; Chen, Y. In silico aided metabolic engineering of *Streptomyces roseosporus* for daptomycin yield improvement. *Appl. Microbiol. Biotechnol.* **2012**, *94*, 637–649. [[CrossRef](#)] [[PubMed](#)]
42. Chemler, J.A.; Fowler, Z.L.; McHugh, K.P.; Koffas, M.A.G. Improving NADPH availability for natural product biosynthesis in *Escherichia coli* by metabolic engineering. *Metab. Eng.* **2010**, *12*, 96–104. [[CrossRef](#)] [[PubMed](#)]
43. Bhan, N.; Xu, P.; Khalidi, O.; Koffas, M.A.G. Redirecting carbon flux into malonyl-CoA to improve resveratrol titers: Proof of concept for genetic interventions predicted by OptForce computational framework. *Chem. Eng. Sci.* **2013**, *103*, 109–114. [[CrossRef](#)]
44. Xu, P.; Ranganathan, S.; Fowler, Z.L.; Maranas, C.D.; Koffas, M.A.G.G. Genome-scale metabolic network modeling results in minimal interventions that cooperatively force carbon flux towards malonyl-CoA. *Metab. Eng.* **2011**, *13*, 578–587. [[CrossRef](#)] [[PubMed](#)]
45. Zhang, Y.; Wang, Y.; Zhou, Z.; Wang, P.; Xi, X.; Hu, S.; Xu, R.R.; Du, G.; Li, J.; Chen, J.; et al. Synthesis of bioengineered heparin by recombinant yeast *Pichia pastoris*. *Green Chem.* **2022**, *24*, 3180–3192. [[CrossRef](#)]
46. Couto, M.R.; Rodrigues, J.L.; Rodrigues, L.R. Cloning, Expression and Characterization of UDP-Glucose Dehydrogenases. *Life* **2021**, *11*, 1201. [[CrossRef](#)] [[PubMed](#)]
47. Karr, C.D. *Identification of a Novel β 1,3-N-Acetylgalactosaminyltransferase Activity and Its Unique β 1,3-GalNAc Homopolymer That Forms the Giardia Cyst Wall*; Biology Northeastern University: Boston, MA, USA, 2009.
48. Lopez, A.B.; Sener, K.; Jarroll, E.L.; Van Keulen, H. Transcription regulation is demonstrated for five key enzymes in *Giardia intestinalis* cyst wall polysaccharide biosynthesis. *Mol. Biochem. Parasitol.* **2003**, *128*, 51–57. [[CrossRef](#)] [[PubMed](#)]
49. Kitagawa, H.; Ujikawa, M.; Sugahara, K. Developmental changes in serum UDP-GlcA:chondroitin glucuronyltransferase activity. *J. Biol. Chem.* **1996**, *271*, 6583–6585. [[CrossRef](#)] [[PubMed](#)]
50. Kitagawa, H.; Ujikawa, M.; Tsutsumi, K.; Tamura, J.I.; Neumann, K.W.; Ogawa, T.; Sugahara, K. Characterization of serum β -glucuronyltransferase involved in chondroitin sulfate biosynthesis. *Glycobiology* **1997**, *7*, 905–911. [[CrossRef](#)] [[PubMed](#)]
51. Rainha, J.; Rodrigues, J.L.; Rodrigues, L.R. CRISPR-Cas9: A powerful tool to efficiently engineer *Saccharomyces cerevisiae*. *Life* **2021**, *11*, 13. [[CrossRef](#)] [[PubMed](#)]
52. Shaw, J.A.; Mol, P.C.; Bowers, B.; Silverman, S.J.; Valdivieso, M.H.; Duran, A.; Cabib, E. The function of chitin synthases 2 and 3 in the *Saccharomyces cerevisiae* cell cycle. *J. Cell Biol.* **1991**, *114*, 111–123. [[CrossRef](#)] [[PubMed](#)]
53. Lesage, G.; Bussey, H. Cell Wall Assembly in *Saccharomyces cerevisiae*. *Microbiol. Mol. Biol. Rev.* **2006**, *70*, 317–343. [[CrossRef](#)] [[PubMed](#)]
54. Orlean, P. Architecture and biosynthesis of the *Saccharomyces cerevisiae* cell wall. *Genetics* **2012**, *192*, 775–818. [[CrossRef](#)] [[PubMed](#)]
55. Klis, F.M.; Mol, P.; Hellingwerf, K.; Brul, S. Dynamics of cell wall structure in *Saccharomyces cerevisiae*. *FEMS Microbiol. Rev.* **2002**, *26*, 239–256. [[CrossRef](#)] [[PubMed](#)]
56. Zhang, Q.; Yao, R.; Chen, X.; Liu, L.; Xu, S.; Chen, J.; Wu, J. Enhancing fructosylated chondroitin production in *Escherichia coli* K4 by balancing the UDP-precursors. *Metab. Eng.* **2018**, *47*, 314–322. [[CrossRef](#)] [[PubMed](#)]
57. Wu, J.; Zhang, Q.; Liu, L.; Chen, X.; Liu, J.; Luo, Q. Recombinant *Escherichia coli* for High Efficiency Production of Fructosylated Chondroitin and Method for Making Thereof. U.S. Patent 10,508,279 B2, 17 December 2019.
58. D’ambrosio, S.; Alfano, A.; Cassese, E.; Restaino, O.F.; Barbutto Ferraiuolo, S.; Finamore, R.; Cammarota, M.; Schiraldi, C.; Cimini, D. Production and purification of higher molecular weight chondroitin by metabolically engineered *Escherichia coli* K4 strains. *Sci. Rep.* **2020**, *10*, 13200. [[CrossRef](#)]
59. Barros, M.H.; Tzagoloff, A. Regulation of the heme A biosynthetic pathway in *Saccharomyces cerevisiae*. *FEBS Lett.* **2002**, *516*, 119–123. [[CrossRef](#)] [[PubMed](#)]
60. Sánchez, B.J.; Zhang, C.; Nilsson, A.; Lahtvee, P.; Kerkhoven, E.J.; Nielsen, J. Improving the phenotype predictions of a yeast genome-scale metabolic model by incorporating enzymatic constraints. *Mol. Syst. Biol.* **2017**, *13*, 935. [[CrossRef](#)] [[PubMed](#)]
61. Entian, K.-D.; Kötter, P. 25 Yeast Genetic Strain and Plasmid Collections. In *Methods in Microbiology*; Stansfield, I., Stark, M.J.R., Eds.; Elsevier: Amsterdam, The Netherlands, 2007; Volume 36, pp. 629–666. ISBN 0123694787.
62. Brachmann, C.B.; Davies, A.; Cost, G.J.; Caputo, E.; Li, J.; Hieter, P.; Boeke, J.D. Designer deletion strains derived from *Saccharomyces cerevisiae* S288C: A useful set of strains and plasmids for PCR-mediated gene disruption and other applications. *Yeast* **1998**, *14*, 115–132. [[CrossRef](#)]
63. Chen, Y.; Partow, S.; Scalcinati, G.; Siewers, V.; Nielsen, J. Enhancing the copy number of episomal plasmids in *Saccharomyces cerevisiae* for improved protein production. *FEMS Yeast Res.* **2012**, *12*, 598–607. [[CrossRef](#)] [[PubMed](#)]
64. Gietz, R.D.; Woods, R.A. Transformation of yeast by lithium acetate/single-stranded carrier DNA/polyethylene glycol method. In *Methods in Enzymology*; Academic Press: New York, NY, USA, 2002; Volume 350, pp. 87–96.
65. Bitter, T.; Muir, H.M. A modified uronic acid carbazole reaction. *Anal. Biochem.* **1962**, *4*, 330–334. [[CrossRef](#)] [[PubMed](#)]
66. Lu, H.; Li, F.; Sánchez, B.J.; Zhu, Z.; Li, G.; Domenzain, I.; Marcišauskas, S.; Anton, P.M.; Lappa, D.; Lieven, C.; et al. A consensus *S. cerevisiae* metabolic model Yeast8 and its ecosystem for comprehensively probing cellular metabolism. *Nat. Commun.* **2019**, *10*, 3586. [[CrossRef](#)] [[PubMed](#)]
67. Rocha, I.; Maia, P.; Evangelista, P.; Vilaça, P.; Soares, S.; Pinto, J.P.; Nielsen, J.; Patil, K.R.; Ferreira, E.C.; Rocha, M. OptFlux: An open-source software platform for in silico metabolic engineering. *BMC Syst. Biol.* **2010**, *4*, 45. [[CrossRef](#)] [[PubMed](#)]

68. Lewis, N.E.; Hixson, K.K.; Conrad, T.M.; Lerman, J.A.; Charusanti, P.; Polpitiya, A.D.; Adkins, J.N.; Schramm, G.; Purvine, S.O.; Lopez-Ferrer, D.; et al. Omic data from evolved *E. coli* are consistent with computed optimal growth from genome-scale models. *Mol. Syst. Biol.* **2010**, *6*, 390. [[CrossRef](#)] [[PubMed](#)]
69. Zitzler, E.; Laumanns, M.; Thiele, L. SPEA2: Improving the Strength Pareto Evolutionary Algorithm. In *TIK Report*; ETH Zurich: Zurich, Switzerland, 2001; pp. 1–21. [[CrossRef](#)]
70. Pereira, V.; Cruz, F.; Rocha, M. MEWpy: A computational strain optimization workbench in Python. *Bioinformatics* **2021**, *37*, 2494–2496. [[CrossRef](#)] [[PubMed](#)]
71. Deb, K.; Pratap, A.; Agarwal, S.; Meyarivan, T. A fast and elitist multiobjective genetic algorithm: NSGA-II. *IEEE Trans. Evol. Comput.* **2002**, *6*, 182–197. [[CrossRef](#)]
72. Mahadevan, R.; Schilling, C.H. The effects of alternate optimal solutions in constraint-based genome-scale metabolic models. *Metab. Eng.* **2003**, *5*, 264–276. [[CrossRef](#)] [[PubMed](#)]

Disclaimer/Publisher’s Note: The statements, opinions and data contained in all publications are solely those of the individual author(s) and contributor(s) and not of MDPI and/or the editor(s). MDPI and/or the editor(s) disclaim responsibility for any injury to people or property resulting from any ideas, methods, instructions or products referred to in the content.